MNRAS **441,** 525–531 (2014) doi:10.1093/mnras/stu419

The role of feedback in shaping the structure of the interstellar medium

A. P. Walker,[1] B. K. Gibson,[1,2]★ K. Pilkington,[1,2] C. B. Brook,[1,3] P. Dutta,[4] S. Stanimirović,[5] G. S. Stinson[6] and J. Bailin[7]

[1]*Jeremiah Horrocks Institute, University of Central Lancashire, Preston PR1 2HE, UK*
[2]*Department of Astronomy & Physics, Institute for Computational Astrophysics, Saint Mary's University, Halifax, NS B3H 3C3, Canada*
[3]*Departamento de Física Teórica, Universidad Autónoma de Madrid, E-28049 Cantoblanco, Madrid, Spain*
[4]*National Centre for Radio Astrophysics, Post Bag 3, Ganeshkhind, Pune 411 007, India*
[5]*Department of Astronomy, University of Wisconsin, 475 North Charter St, Madison, WI 53706, USA*
[6]*Max-Planck-Institut für Astronomie, Königstuhl 17, D-69117 Heidelberg, Germany*
[7]*Department of Physics & Astronomy, University of Alabama, Tuscaloosa, AL 35487-0324, USA*

Accepted 2014 March 3. Received 2014 February 28; in original form 2013 June 30

ABSTRACT

We present an analysis of the role of feedback in shaping the neutral hydrogen (H I) content of simulated disc galaxies. For our analysis, we have used two realizations of two separate Milky Way-like ($\sim L\star$) discs – one employing a conservative feedback scheme (McMaster Unbiased Galaxy Survey), the other significantly more energetic [Making Galaxies In a Cosmological Context (MaGICC)]. To quantify the impact of these schemes, we generate zeroth moment (surface density) maps of the inferred H I distribution; construct power spectra associated with the underlying structure of the simulated cold interstellar medium, in addition to their radial surface density and velocity dispersion profiles. Our results are compared with a parallel, self-consistent, analysis of empirical data from The H I Nearby Galaxy Survey (THINGS). Single power-law fits ($P \propto k^{\gamma}$) to the power spectra of the stronger feedback (MaGICC) runs (over spatial scales corresponding to ∼0.5 to ∼20 kpc) result in slopes consistent with those seen in the THINGS sample ($\gamma \sim -2.5$). The weaker feedback (MUGS) runs exhibit shallower power-law slopes ($\gamma \sim -1.2$). The power spectra of the MaGICC simulations are more consistent though with a two-component fit, with a flatter distribution of power on larger scales (i.e. $\gamma \sim -1.4$ for scales in excess of ∼2 kpc) and a steeper slope on scales below ∼1 kpc ($\gamma \sim -5$), qualitatively consistent with empirical claims, as well as our earlier work on dwarf discs. The radial H I surface density profiles of the MaGICC discs show a clear exponential behaviour, while those of the MUGS suite are essentially flat; both behaviours are encountered in nature, although the THINGS sample is more consistent with our stronger (MaGICC) feedback runs.

Key words: ISM: structure – galaxies: evolution – galaxies: formation – galaxies: spiral.

1 INTRODUCTION

The feedback of energy into the interstellar medium (ISM) is a fundamental factor in shaping the morphology, kinematics, and chemistry of galaxies, both in nature and in their simulated analogues (e.g. Thacker & Couchman 2000; Governato et al. 2010; Schaye et al. 2010; Hambleton et al. 2011; Brook et al. 2012; Durier & Dalla Vecchia 2012; Scannapieco et al. 2012; Hopkins et al. 2013, and references therein). Perhaps the single most frustrating impediment to realizing accurate realizations of simulated galaxies is the spatial 'mismatch' between the sub-pc scale on which star formation and feedback operate, and the 10–100 s of pc scale accessible to modellers within a cosmological framework. Attempts to better constrain 'subgrid' physics, on a macroscopic scale, have driven the field for more than a decade and will likely continue to do so into the foreseeable future.

The efficiency and mechanism by which energy from massive stars [both explosive energy deposition from supernovae (SNe) and pre-explosion radiation energy], cosmic rays, and magnetic fields couples to the ISM can be constrained indirectly via an array of empirical probes, including (but not limited to) stellar halo (Brook et al. 2004) and disc (Pilkington et al. 2012a) metallicity distribution functions, statistical measures of galaxy light compactness, asymmetry, and clumpiness (Hambleton et al. 2011), stellar disc age–velocity dispersion relations (House et al. 2011), rotation curves and density profiles of dwarf galaxies (Macciò et al. 2012), low- and high-redshift 'global' scaling relations (Brook et al. 2012),

★ E-mail: brad.k.gibson@gmail.com

background quasar probes of the ionized circumgalactic medium (Stinson et al. 2012), and the spatial distribution of metals (e.g. abundance gradients and age–metallicity relations) throughout the stellar disc (Pilkington et al. 2012b; Gibson et al. 2013).

In Pilkington et al. (2011), we explored an alternate means by which to assess the efficacy of energy feedback schemes within a cosmological context: specifically, the predicted distribution of structural 'power' encoded within the underlying cold gas of late-type *dwarf* galaxies. Empirically, star-forming dwarfs present steep spatial power-law spectra ($P \propto k^{\gamma}$) for their cold gas, with $\gamma < -3$ on spatial scales $\lesssim$1 kpc (Stanimirovic et al. 1999; Combes et al. 2012), consistent with the slope expected when H I density fluctuations dominate the ISM structure, rather than turbulent velocity fluctuations (which dominate when isolating 'thin' velocity slices). Our simulated (dwarf) disc galaxies showed similarly steep ISM power-law spectra, albeit deviating somewhat from the simple, single, power law seen by Stanimirovic et al.

In comparison, the cold gas of late-type giant galaxies appears to possess a more complex distribution of structural power. Dutta et al. (2013) demonstrate that while such massive discs also present comparably steep (if not steeper) power spectra on smaller scales ($\gamma \sim -3$, for $\lesssim$1 kpc), there is a strong tendency for the power to 'flatten' to significantly shallower slopes on larger scales ($\gamma \sim -1.5$, for $\gtrsim$2 kpc). Dutta et al. propose a scenario in which the steeper power-law component is driven by three-dimensional turbulence in the ISM on scales smaller than a given galaxy's scaleheight, while the flatter component is driven by two-dimensional turbulence in the plane of the galaxy's disc.

In what follows, we build upon our earlier work on dwarf galaxies (Pilkington et al. 2011), utilizing the Fourier domain approach outlined by Stanimirovic et al. (1999), but now applied to a set of four simulated massive ($\sim L\star$) disc systems. The simulations have each been realized with both conventional (i.e. moderate) and enhanced (i.e. strong/efficient) energy feedback. The impact of the feedback prescriptions upon the distribution of power in the ISM of their respective neutral hydrogen (H I) discs will be used, in an attempt to constrain the uncertain implementation of subgrid physics. H I moment maps will be generated for each simulation and (for consistency) massive disc from The H I Nearby Galaxy Survey (THINGS; Walter et al. 2008), to make a fairer comparison with the observational data.

In Section 2, the basic properties of the simulations are reviewed, including the means by which the H I moment maps, and associated Fourier domain power spectra, were analysed. The resulting radial surface density profiles, velocity dispersion profiles, and distributions of power in the corresponding cold interstellar media are described in Section 3. Our conclusions are presented in Section 4.

2 METHOD

2.1 Simulations

Two $\sim L\star$ disc galaxies (g1536; g15784), drawn from the McMaster Unbiased Galaxy Survey (MUGS; Stinson et al. 2010) and realized with the smoothed particle hydrodynamics (SPH) code GASOLINE (Wadsley, Stadel & Quinn 2004) form the primary inputs to our analysis.[1] Two variants for each disc were generated, one employing 'conventional' feedback (MUGS) and one using our 'enhanced' feedback scheme (MaGICC: Making Galaxies In a Cosmological Context; Brook et al. 2012; Stinson et al. 2012).[2] These four massive disc simulations are referred to henceforth as g1536-MUGS, g1536-MaGICC, g15784-MUGS, and g15784-MaGICC, and form the primary suite to which the subsequent analysis has been employed. To provide a bridge to our earlier study of the ISM power spectra of dwarf galaxies (Pilkington et al. 2011), we have analysed an ancillary set of three simulated low-mass discs (Section 3.4). An in-depth discussion of the MUGS and MaGICC star formation and feedback prescriptions is provided in the aforementioned works, although a brief summary of the key characteristics follows now.

The MUGS runs assume a thermal feedback scheme in which 4×10^{50} erg per SN is made available to heat the surrounding ISM ('conventional'), while the MaGICC runs use 10^{51} erg per SN ('enhanced'). The MUGS simulations employ a Kroupa, Tout & Gilmore (1993) initial mass function, while MaGICC use the more 'top-heavy' Chabrier (2003) form.[3] Radiation energy feedback from massive stars during their pre-SN phase (lasting $\sim$4 Myr) is included in the MaGICC runs, although it should be emphasized that the effective coupling efficiency is <1 per cent (Brook et al. 2012; Stinson et al. 2013). For both MUGS and MaGICC, cooling is disabled for gas particles situated within a blast region of size $\sim$100 pc, for a time period of $\sim$10 Myr. Star formation is restricted to regions which are both sufficiently cool and dense (MUGS: >1 cm^{-3}; MaGICC: >9 cm^{-3}). Metal diffusion (Shen, Wadsley & Stinson 2010) is included in all runs.

Supplementing the above four massive disc simulations, we have included three lower mass dwarf discs: (a) SG2 and SG3 (Brook et al. 2012) were realized with the same star formation and feedback schemes as the MaGICC versions of g1536 and g15784, respectively; the only difference lies in their initial conditions, where the former have been 'scaled down' by an order of magnitude in mass; (b) DG1 (Governato et al. 2010), the low-mass dwarf that formed the basis of our earlier work (Pilkington et al. 2011).

2.2 Analysis

The analysis which follows is based upon a comparison of the H I gas properties of the MUGS+MaGICC simulations with their empirical 'analogues', drawn from THINGS (Walter et al. 2008). We 'view' the simulations face-on and restrict the comparison to massive discs from THINGS which are also close to face-on. In practice, this has meant limiting the analysis to the same subsample as that used by Dutta et al. (2013). In contrast, our earlier work (Pilkington et al. 2011) focused on low-mass dwarf galaxies, rather than massive discs; in that study, we found that the index of the simulated ISM power spectrum (γ, where $P \propto k^{\gamma}$) was consistent, to first order, with that observed in dwarfs (on spatial scales $\lesssim$1 kpc) such as the Small Magellanic Cloud (i.e. $\gamma \sim -3.2$). Besides determining the slope of the ISM power spectra for our new suite of massive disc galaxy simulations, we will present the radial H I surface density

[1] The role of feedback in shaping the abundance gradients, metallicity distribution functions, and age–metallicity relations of these same four realizations has been presented recently by Gibson et al. (2013).

[2] To link the simulation nomenclature with their earlier appearances in the literature, the MUGS variants of g1536 and g15784 are as first presented by Stinson et al. (2010), and analysed subsequently by Pilkington et al. (2012b) and Calura et al. (2012), while the MaGICC variant of g1536 corresponds to the 'fiducial' run in Stinson et al. (2013) (itself, essentially the same as SG5LR, as first described by Brook et al. 2012).

[3] The MUGS runs assumed that the global metallicity $Z \equiv$ O+Fe, while those of MaGICC assume $Z \equiv$ O+Fe+C+N+Ne+Mg+Si.

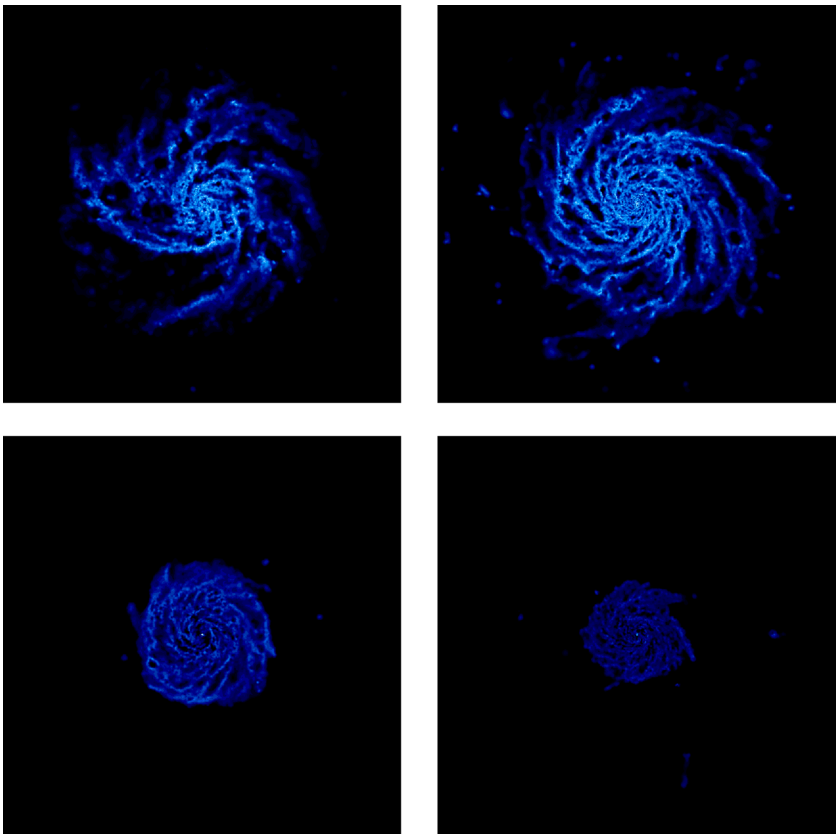

Figure 1. Zeroth-moment H I maps for our four simulated $\sim L\star$ late-type discs: g1536-MaGICC (upper left); g15784-MaGICC (upper right); g1536-MUGS (bottom left); g15784-MUGS (bottom right). Each panel spans 100 × 100 kpc, with a column density range of 10^{19} to 10^{21} cm^{-2} (comparable to the limits imposed by 21 cm surveys such as THINGS).

and velocity dispersion profiles and contrast them with empirical data from the literature, in a further attempt to shed light on the role of feedback in shaping their characteristics.

In what follows, we make use of zeroth- (surface density) and second- (velocity dispersion) moment maps of each simulation's H I distribution (viewed, face-on), realized with the image processing package TIPSY.[4] The redshift $z = 0$ snapshots for each galaxy are first centred and aligned such that the angular momentum vector of the disc is aligned with the z-axis, and the neutral hydrogen fraction of each SPH particle inferred under the assumption of combined photo- and collisional-ionization equilibrium. From the zeroth- (second-) moment maps, radial H I surface density (velocity dispersion) profiles were generated for each simulation and (near) face-on, late-type disc from THINGS. Individual results for each will be presented in Section 3. It is worth noting that out of the THINGS galaxies presented in Fig. A1, NGCs 3031, 5236, 5457, and 6946 are more extended than the Very Large Array primary beam, resulting potentially in missing larger scale information (Walter et al. 2008).

After Stanimirovic et al. (1999) and Pilkington et al. (2011), the Fourier transform of each of the aforementioned zeroth-moment H I maps (both simulations and empirical THINGS data) was taken, with circular annuli in Fourier space then employed to derive the average power in the structure of the ISM on different spatial scales.

[4] www-hpcc.astro.washington.edu/tools/tipsy/tipsy.html

3 RESULTS

3.1 Moment maps

The zeroth-moment H I maps for our four simulated $\sim L\star$ late-type discs are shown in Fig. 1, with the two MaGICC (MUGS) variants shown in the upper (lower) panels. Each panel spans 100 × 100 kpc. The 'dynamic range' in H I column density in each panel is $\sim 10^{19}$ to $\sim 10^{21}$ cm^{-2} – i.e. (roughly) the current observational lower and upper limits for H I (21 cm) detection (Bigiel et al. 2008).

Even a cursory inspection of Fig. 1 suggests that the enhanced feedback employed within MaGICC results in significantly more extended H I discs, relative to the conventional feedback treatment within MUGS. Similarly, at these column densities, the eye is drawn to the enhanced structure on larger scales seen in the MaGICC runs (relative to the more locally 'confined' structure seen in MUGS). Both points will be returned to below in a more quantitative sense.

3.2 Radial surface density profiles

From the face-on moment zero maps of Fig. 1, radial H I surface density profiles were generated. These are reflected in Fig. 2 with the MUGS and MaGICC variants for g1536 (g15784) shown in the left-hand (right-hand) panel. As for Fig. 1, the dynamic range has been limited to $\gtrsim 10^{19}$ cm^{-2} ($\gtrsim 10^{5}$ M$_{\odot}$ kpc^{-2}), to reflect the (typical) limiting 21 cm detection limit in surveys such as THINGS;

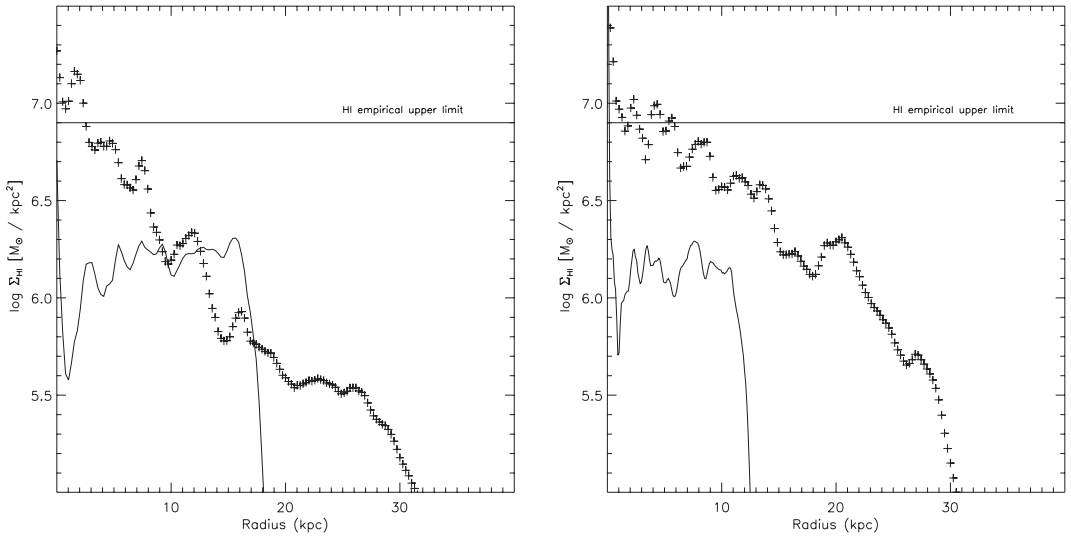

Figure 2. Radial H I surface density profiles for the g1536 (left-hand panel) and g15784 (right-hand panel) simulations. The plus symbols represent the MaGICC runs and the solid lines correspond to the MUGS runs. The solid horizontal line in each panel corresponds to the empirical H I upper limit from Bigiel et al. (2008).

conversely, the horizontal line in each panel corresponds to the empirical H I upper limit (also from THINGS) of $\sim 10^{6.9}$ $M_\odot$ kpc^{-2}.

The MaGICC discs (plus symbols in both panels) possess exponential surface density profiles (in H I) with ∼6–8 kpc scalelengths. Conversely, the MUGS realizations are clearly more 'compact', with essentially 'flat' radial H I surface density profiles (each with $\sim 10^{20}$ cm^{-2}, independent of galactocentric radius), with an extremely 'sharp' H I edge at ∼12–15 kpc. At a limiting H I (21 cm) column density of $\sim 10^{19}$ cm^{-2}, the MaGICC discs are ∼2–3 times more extended than their MUGS analogues. At first glance, in terms of both radial dependence and amplitude, the H I surface density profiles of the MaGICC discs resemble very closely those shown in fig. 23 of O'Brien et al. (2010). It is important to bear in mind though that the O'Brien et al. profiles were inferred (necessarily) from observations of edge-on discs. Our analysis of the simulations is restricted to face-on orientations, and so a fairer comparison would be to the sample of Bigiel & Blitz (2012), who derived both H I and H_2 surface density profiles for a sample of face-on galaxies observed by THINGS.

Bigiel & Blitz (2012) show that the H I in such disc galaxies is distributed more uniformly, in terms of surface density, out to ∼10 kpc, with (roughly) only a factor of ∼3 decline in going to a galactocentric radius of ∼20 kpc. This is consistent with the flatter gradient seen for the MUGS simulations, albeit the issue of their aforementioned overly truncated 'edges' remains. Because we cannot resolve the transition from H I to H_2 in our simulations, some fraction of what is labelled as 'H I' in Fig. 2 (at least within the inner 5–10 kpc, for the MaGICC simulations, where the surface density is close to, or exceeds, the empirical upper limit for H I in nature) could certainly be misidentified H_2, and so our inner gradients would be somewhat flatter than presented and therefore more consistent with the profiles of Bigiel and Blitz for radii $\lesssim$10 kpc. Our predicted H I surface density gradients in the ∼10–20 kpc range are (on average) somewhat steeper than the typical galaxy from Bigiel and Blitz (in the same radial range – see their fig. 1a) but certainly lie within $\sim 1\sigma$ of the distribution. In that sense, the extended nature and (outer disc) exponential profiles of the MaGICC simulations are more consistent with those encountered in nature.

3.3 Radial velocity dispersion profiles

The radial H I velocity dispersion profiles derived from the second-moment maps (Fig. 3) present fairly 'flat' trends with increasing galactocentric distance, save for perhaps g15784, with σ decreasing typically by ∼50 per cent in going from the inner disc to a galactocentric radius of ∼10 kpc; the profiles for the dwarfs (SG2 and SG3) are flat over this radial range, consistent with the dwarfs shown in fig. 3 of Pilkington et al (2011). Here, as the second-moment maps are for face-on viewing angles, the velocity dispersions quoted in Fig. 3 are equivalent to σ_W. We are only showing the velocity dispersion profiles within the star-forming parts of the discs (i.e. radii

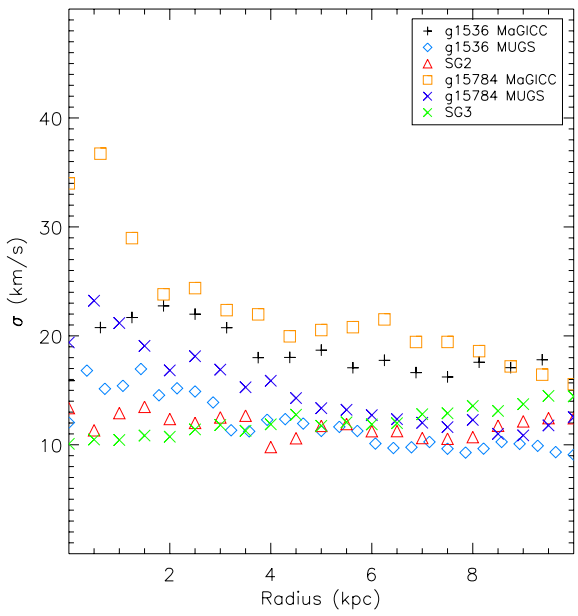

Figure 3. Line-of-sight velocity dispersion profiles for the H I within the face-on representations of g1536-MaGICC (black plus symbols); g1536-MUGS (blue diamonds); g15784-MaGICC (red triangles); g15784-MUGS (orange squares); SG2 (blue crosses), and SG3 (green crosses).

$\lesssim r_{25}$ for the massive MaGICC and MUGS discs, and $\lesssim 2r_{25}$ for the lower mass dwarfs SG2 and SG3, where r_{25} is the isophotal radius corresponding to 25 mag arcsec^{-2}). As such, the dispersions being ∼20–100 per cent higher than the 'characteristic' value outside the star-forming disc (∼10 km s^{-1}; Tamburro et al. 2009) is not entirely unexpected.

The three main conclusions to take from this part of the analysis are that (i) the profiles and amplitudes for the velocity dispersions of the cold gas within the star-forming region of the four massive MUGS and MaGICC discs overlap with those encountered in nature (fig. 1 of Tamburro et al. 2009); (ii) the flat profiles of the two dwarfs (SG2 and SG3) are more problematic, consistent with the conclusions of Pilkington et al. (2011), and reflecting a limitation of our inability to resolve molecular hydrogen processes on these scales; (iii) the amplitudes of the MaGICC variants, relative to their MUGS counterparts, are ∼50 per cent higher (although both are within the range encountered in nature); such a result is not entirely unexpected, given the significantly enhanced feedback associated with the MaGICC runs.

3.4 Power spectra

As noted in Section 2.2, power spectra were derived from each of the simulated and empirical (THINGS) H I moment-zero maps, by averaging in circular annuli in frequency space after Fourier transforming the images. The technique is identical to that employed by Stanimirovic et al. (1999) and Pilkington et al. (2011). While alternate approaches certainly exist (cf. Dutta et al. 2013), we are more concerned here with adopting a homogeneous approach for both the simulations and the data, rather than necessarily intercomparing the various techniques available.

Fig. 4 shows the power spectra for both the MaGICC and MUGS variants of g1536 and g15784 simulations, as well as their respective dwarf galaxy analogues, SG2 and SG3. For each of the four massive discs' spectra, single power-law fits are shown (solid curves) for the spatial scales over which the fits were derived (∼0.6–2 kpc). It should be emphasized that the lower limit on the spatial scale over which these fits were made corresponds to twice the softening length employed in the simulations; while an argument could be made to extending to somewhat smaller scales, we felt it prudent to be conservative in our analyses. What can hopefully be appreciated from a cursory analysis of Fig. 4 is the relatively enhanced power on sub-kpc scales seen in MUGS (conventional feedback) realizations, compared with their MaGICC (enhanced feedback) analogues. This is reflected in the single power-law slopes itemized in the inset to the panel (which are weighted heavily by the more 'numerous' higher frequency 'bins' on sub-kpc scales), which are meant to be illustrative here, rather than represent the formal 'best fit' to the data. Broadly speaking, the power spectra are roughly an order of magnitude steeper when using the MaGICC feedback scheme, as opposed to that of MUGS – i.e. it appears that the stronger feedback shifts the ISM power from predominantly 'small' ($\lesssim$1 kpc) to 'large' ($\gtrsim$2 kpc) spatial scales.

We next extended our analysis to lower mass, late-type systems, including the two dwarf variants to g1536-MaGICC and g15784-MaGICC (referred to as SG2 and SG3, as per Brook et al. 2012). We also performed an independent re-analysis of the dwarf (DG1) that formed the basis of our earlier work (Pilkington et al. 2011). The inclusion of these three 'dwarfs' allows us to push the analysis to somewhat smaller spatial scales, while still working within a framework of 'enhanced' feedback. The power spectra for all seven systems are shown in Fig. 4. An important conclusion to be drawn

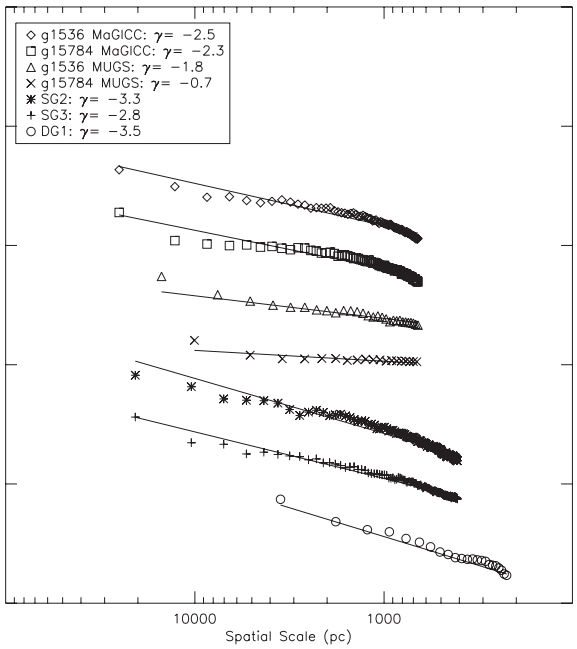

Figure 4. Power spectra for the four ∼$L\star$ MaGICC and MUGS simulations (upper four spectra), two 'dwarf' variants of g1536 and g15784 (SG2 and SG3, respectively), and the low-mass dwarf DG1, from Pilkington et al. (2011). The inset within the panel links the symbol with the relevant simulation. The ordinate represents arbitrary units of spatial power, as the relative distribution (rather than absolute) is the focus of this work; each spectrum has been offset with respect to the next, for ease of viewing.

from this figure (and associated quoted single power-law fits within the inset to the panel) is that on ∼sub-kpc scales, the power spectra slopes of the three dwarfs (SG2, SG3, and DG1) are steeper ($-3.5 \lesssim \gamma \lesssim -3$) than their more massive analogues.

We then compared the predicted power spectra from the two ∼$L\star$ discs realized with the enhanced MaGICC feedback scheme, with those derived from galaxies from the THINGS data base; the full data base is shown in Fig. A1, but for succinctness, we only show the power spectra for NGC 628 and 3184 (which were chosen, in part, because they were the closest to face-on, matching, by construct, the MaGICC simulations), alongside the MaGICC discs, in Fig. 5. In terms of formal single power-law fits to these spectra, the MaGICC and (selected) THINGS galaxies are very similar (as shown by the quoted slopes within the inset to the panel). Having said that, as already alluded to in relation to Fig. 4, the MaGICC spectra do not appear entirely consistent with a single power law, instead presenting evidence for something of a 'break' in the structural power, on the scales of ∼1–2 kpc (being flatter on larger scales, and steeper on smaller scales, a point to which we return below).

Inspection of Figs 4 and 5 suggests that single power-law fits are not necessarily the best option. In Fig. 6, we show the result of performing two-component fits to both the MaGICC data and a selected galaxy from THINGS (NGC 2403, chosen as it is the THINGS galaxy whose power spectrum looks like it would suit a two-component fit best). In a qualitative sense, the behaviour is not dissimilar – i.e. both the MaGICC simulations and NGC 2403 show flatter power spectra on larger scales, compared with smaller scales, although the transition from 'flat' to 'steep' occurs at ∼2 kpc in the simulations, as opposed to ∼0.5 kpc in NGC 2403. This seems to be consistent with the idea posed by Dutta et al. (2013) that there is a steep power-law component on smaller scales driven

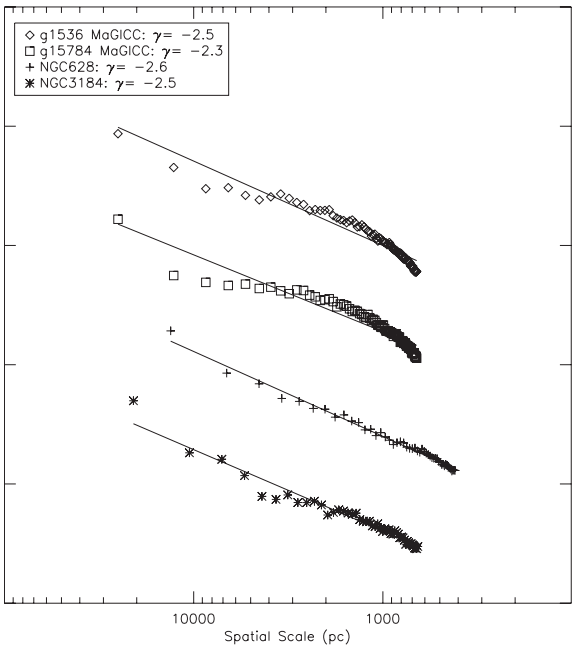

Figure 5. Power spectra for the two MaGICC simulations and two selected from the empirical THINGS data set (NGC 628 and 3184). All other details are as per the caption to Fig. 4.

by three-dimensional turbulent motions, which flattens at larger spatial scales. At these larger scales, two-dimensional turbulent motions begin to dominate within the plane of the galactic disc. The steepening of the power spectra on small spatial scales observed in the power spectra of the MaGICC large discs is also seen in work undertaken by Elmegreen, Kim & Staveley-Smith (2001) in their work on the Large Magellanic Cloud.

Power spectra have been generated for the 17 THINGS galaxies employed in the analysis of Dutta et al. (2013); these are provided in the accompanying appendix as Fig. A1. The majority have slopes of the order of $\gamma \sim -2.3$ to -2.8, with two exceptions: NGC 3031 ($\gamma \sim -0.9$) and NGC 3521 ($\gamma \sim -3.3$). Much as for the simulations, the point associated with the largest spatial scales in each panel should be viewed with some skepticism, as edge effects do come into play (i.e. the 'edge' of the H I disc is 'seen' as a high power 'scale' against an almost noise-free background).

4 CONCLUSIONS

We have presented an analysis of the cold gas and H I content of simulated discs with both 'standard' (MUGS) and 'enhanced' (MaGICC) energy feedback schemes, as well as re-scaled dwarf variants of the massive (MaGICC) simulations.

Radial density profiles were generated for the MUGS and MaGICC $\sim L\star$ variants of g1536 and g15784 (Fig. 2). These were generated using their respective zeroth H I moment maps; the weaker feedback associated with MUGS resulted in very flat radial H I distributions, with sharp cut-offs at galactocentric radii of ∼12–15 kpc, while the stronger feedback associated with MaGICC resulted in H I discs with exponential surface density profiles (with scalelengths of ∼6–8 kpc) which were ∼2–3 times more extended (at an H I column density limit of $\sim 10^{19}$ cm^{-2}). The exponential profiles exhibited by the enhanced feedback runs are consistent with the typical profile observed in nature (Bigiel et al. 2008; O'Brien, Freeman & van der Kruit 2010). The majority of the THINGS radial density profiles show evidence of exponential components, indicating that the MaGICC simulations distribute the column density in a way that better matches observational evidence.

The power spectra generated for the massive ($\sim L\star$) discs with enhanced (MaGICC) feedback are steeper than their weaker (MUGS) feedback counterparts. In other words, the stronger feedback shifts the power in ISM from smaller scales to larger scales. Forcing a single-component power law to the MaGICC spectra yields slopes consistent with similarly forced single-component fits to the empirical THINGS spectra, also well-described by a single-component power law; having said that, the MaGICC spectra are more consistent with a two-component structure, with a steeper slope on sub-kpc spatial scales, flattening to shallower slopes on larger scales. The massive discs realized with the MUGS feedback scheme are both shallower than MaGICC, but also well fitted with a single power law across all spatial scales. The dwarf galaxies realized in our work with enhanced feedback possess steeper slopes than their more massive counterparts, with values that are in agreement with Stanimirovic et al. (1999) and Pilkington et al. (2011).

It is arguable that several of the THINGS power spectra warrant multiple-component fits (namely NGC 2403, 3031, 3184, 3198,

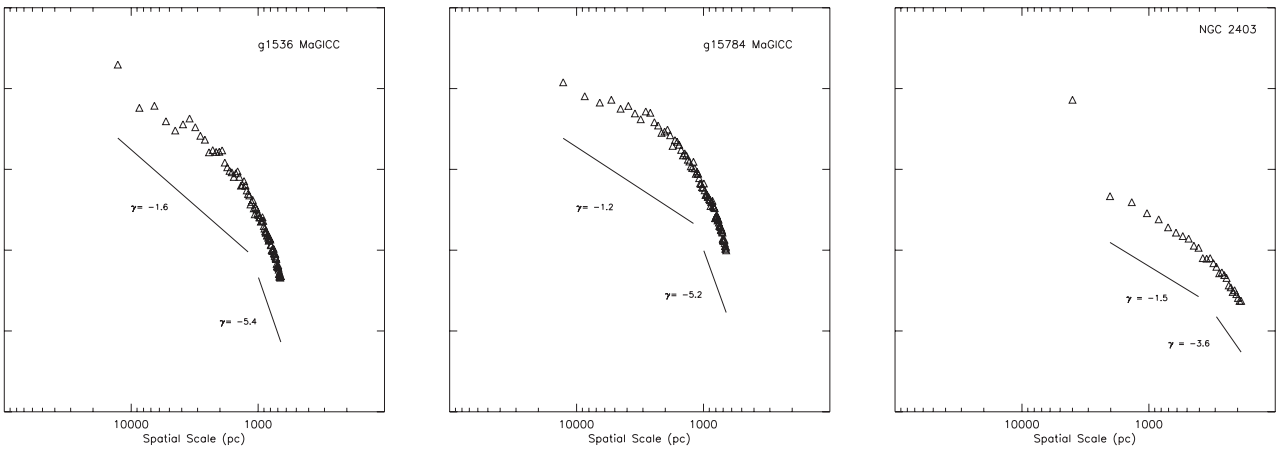

Figure 6. Power spectra of g1536-MaGICC, g15784-MaGICC, and NGC 2403, respectively (from left to right). Each spectrum appears (in a qualitative sense) inconsistent with a single power-law fit; two-component fits, with a shallower (steeper) slope on larger (smaller) scales, are suggested, although the 'knee' in the spectra occurs on different scales for the simulations (∼2 kpc), as opposed to that of NGC 2403 (∼0.5 kpc).

and 7793) and the multicomponent fits performed on NGC 2403, and the two large disc MaGICC galaxy power spectra indicate that the large-scale slopes agree well, whereas the small-scale slopes differ largely. This indicates that the MaGICC feedback scheme distributes H I structures on a scale that is comparable to those of observational results, but there is a lack of small-scale structure. It is apparent that there is no 1:1 match to the THINGS data from either the MUGS or MaGICC feedback schemes, but MaGICC appears to be far better than the MUGS feedback scheme from a single-component fit in an average sense. The lack of a 1:1 relation may be largely due to the challenges in converting from 'cold gas' to 'H I' as well as a lack of exactly face-on systems observed in nature and in the THINGS survey.

ACKNOWLEDGEMENTS

BKG acknowledges the support of the UK Science & Technology Facilities Council (ST/J001341/1). KP acknowledges the support of STFC through its PhD Studentship programme (ST/F007701/1). CBB acknowledges the support of the MINECO (Spain) Grant AYA2012-31101. We also acknowledge the generous allocation of resources from STFCs DiRAC Facility (COSMOS: Galactic Archaeology), the DEISA consortium, co-funded through EU FP6 project RI-031513 and the FP7 project RI-222919 (through the DEISA Extreme Computing Initiative), the PRACE-2IP Project (FP7 RI-283493), and the University of Central Lancashires High Performance Computing Facility.

REFERENCES

Bigiel F., Blitz L., 2012, ApJ, 756, 183
Bigiel F., Leroy A., Walter F., Brinks E., de Blok W. J. G., Madore B., Thornley M. D., 2008, AJ, 136, 2846
Brook C. B., Kawata D., Gibson B. K., Flynn C., 2004, MNRAS, 349, 52
Brook C. B., Stinson G., Gibson B. K., Wadsley J., Quinn T., 2012, MNRAS, 424, 1275
Calura F. et al., 2012, MNRAS, 427, 1401
Chabrier G., 2003, PASP, 115, 763
Combes F. et al., 2012, A&A, 539, A67
Durier F., Dalla Vecchia C., 2012, MNRAS, 419, 465
Dutta P., Begum A., Bharadwaj S., Chengalur J. N., 2013, New Astron., 19, 89
Elmegreen B. G., Kim S., Staveley-Smith L., 2001, ApJ, 548, 749
Gibson B. K., Pilkington K., Brook C. B., Stinson G. S., Bailin J., 2013, A&A, 554, A47
Governato F. et al., 2010, Nature, 463, 203
Hambleton K. M., Gibson B. K., Brook C. B., Stinson G. S., Conselice C. J., Bailin J., Couchman H., Wadsley J., 2011, MNRAS, 418, 801
Hopkins P. F., Cox T. J., Hernquist L., Narayanan D., Hayward C. C., Murray N., 2013, MNRAS, 430, 1901
House E. L. et al., 2011, MNRAS, 415, 2652
Kroupa P., Tout C. A., Gilmore G., 1993, MNRAS, 262, 545
Macciò A. V., Stinson G., Brook C. B., Wadsley J., Couchman H. M. P., Shen S., Gibson B. K., Quinn T., 2012, ApJ, 744, L9
O'Brien J. C., Freeman K. C., van der Kruit P. C., 2010, A&A, 515, A62
Pilkington K. et al., 2011, MNRAS, 417, 2891
Pilkington K. et al., 2012a, MNRAS, 425, 969
Pilkington K. et al., 2012b, A&A, 540, A56
Scannapieco C. et al., 2012, MNRAS, 423, 1726
Schaye J. et al., 2010, MNRAS, 402, 1536
Shen S., Wadsley J., Stinson G., 2010, MNRAS, 407, 1581
Stanimirovic S., Staveley-Smith L., Dickey J. M., Sault R. J., Snowden S. L., 1999, MNRAS, 302, 417
Stinson G. S., Bailin J., Couchman H., Wadsley J., Shen S., Nickerson S., Brook C., Quinn T., 2010, MNRAS, 408, 812
Stinson G. S. et al., 2012, MNRAS, 425, 1270
Stinson G. S., Brook C., Macciò A. V., Wadsley J., Quinn T. R., Couchman H. M. P., 2013, MNRAS, 428, 129
Tamburro D., Rix H.-W., Leroy A. K., Mac Low M.-M., Walter F., Kennicutt R. C., Brinks E., de Blok W. J. G., 2009, AJ, 137, 4424
Thacker R. J., Couchman H. M. P., 2000, ApJ, 545, 728
Wadsley J. W., Stadel J., Quinn T., 2004, New Astron., 9, 137
Walter F., Brinks E., de Blok W. J. G., Bigiel F., Kennicutt R. C., Thornley M. D., Leroy A., 2008, AJ, 136, 2563

APPENDIX A

We present here the ISM power spectra for the 17 THINGS galaxies used in this work. The inset to each panel includes the galaxy name, the weighting scheme employed (RO = robust), and the best-fitting (single-component) power-law slope.

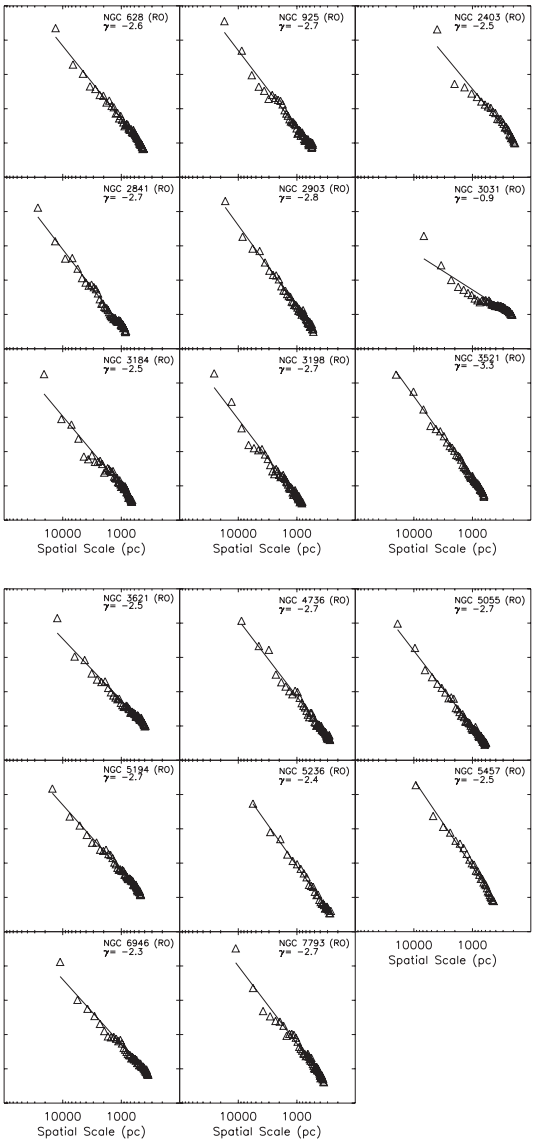

Figure A1. Power spectra for all the THINGS galaxies analysed in this work; names of the galaxies are listed in their corresponding plots along with the power-law slope value. The power-law slope is plotted over the points as a solid line.

This paper has been typeset from a TEX/LATEX file prepared by the author.